Polarized Electron-Electron Scattering at GeV Energies*

P. S. Cooper, M. J. Alguard, R. D. Ehrlich, V. W. Hughes, H. Kobayakawa,† J. S. Ladish,‡ M. S. Lubell, N. Sasao, K. P. Schüler,§ and P. A. Souder
J. W. Gibbs Laboratory, Yale University, New Haven, Connecticut 06520

and

G. Baum and W. Raith
University of Bielefeld, Bielefeld, West Germany

and

K. Kondo‖
University of Tokyo, Tokyo, Japan

and

D. H. Coward, R. H. Miller, C. Y. Prescott, D. J. Sherden, and C. K. Sinclair
Stanford Linear Accelerator Center, Stanford, California 94305
(Received 21 April 1975)

The longitudinal polarization of the new Yale University–Stanford Linear Accelerator Center polarized-electron beam has been determined at laboratory energies between 6.47 and 19.40 GeV. Spin-dependent elastic electron-electron scattering (Møller scattering) has been found to be a practical technique for polarization measurements at high energies. The results are consistent with the energy and angular dependence predicted by quantum electrodynamics and with an energy-independent beam polarization of 0.76 ± 0.03.

Beams of polarized high-energy electrons will provide unique information about the spin-dependent structure of the electromagnetic and weak hadron currents.[1,2] The first such beam has recently been accelerated from the Yale University–Stanford Linear Accelerator Center (SLAC) polarized-electron source (PEGGY) to high energies and has been found to possess a reversible, energy-independent polarization of 0.76 ± 0.03. The SLAC 8-GeV/c spectrometer[3] was used to detect the scattered electrons in a single-arm Møller-scattering experiment in which both the electron target and the incident beam were longitudinally polarized. The measured asymmetry $A = [\sigma(\uparrow\downarrow) - \sigma(\uparrow\uparrow)]/[\sigma(\uparrow\downarrow) + \sigma(\uparrow\uparrow)]$, where $\sigma(\uparrow\downarrow)$ and $\sigma(\uparrow\uparrow)$ are, respectively, the cross sections for beam and target polarization directions antiparallel and parallel, was used in conjunction with the known target polarization to determine the polarization of the incident high-energy electron beam.

PEGGY, described in detail elsewhere,[4] produces longitudinally polarized electrons by photoionization of a state-selected Li^6 atomic beam, with the sense of polarization determined by the direction of a 200-G longitudinal magnetic field applied at the photoionization region. The photoelectrons, extracted at an energy of ~70 keV, are transported to the SLAC injector. Measurements carried out by Mott scattering at 70 keV have shown that the polarization of the electrons leaving PEGGY is 0.8 ± 0.1.

After acceleration to high energy[5] the beam is deflected by 24.5° into the experimental area. This 24.5° magnetic bend causes the spin to precess relative to the momentum by an amount $\theta_a = \gamma a \pi (24.5°/180°)$, where γ is the ratio of the electron energy to the electron mass and $a = (g-2)/2$ is the electron g-factor anomaly. If θ_a is restricted to multiples of π in order to maintain longitudinal polarization, the useful beam energies are restricted to multiples of $E_0 = 3.237$ GeV. Thus at 3.237 GeV the spin precesses by π relative to the momentum; at 6.474 GeV, by 2π; etc. During this experiment the polarized beam delivered to the experimental area varied between 2×10^7 and 7×10^7 electrons per pulse at repetition rates up to 180 pulses/sec. Since the completion of the experiment, modifications to PEGGY have led to an increased intensity of 8×10^8 electrons per pulse.

Møller scattering, which has been used at much lower energies to determine the helicity of electrons from β decay[6] and muon decay,[7] was chosen to determine the high-energy beam polarization because the cross section and analyzing power are large and the process is purely quantum elec-

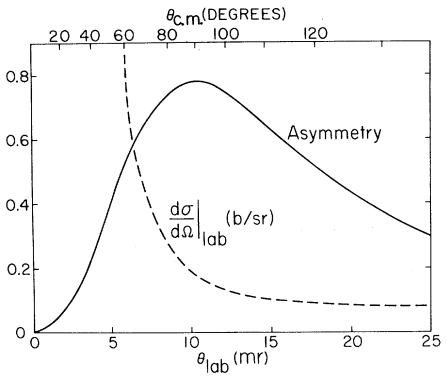

FIG. 1. The Møller asymmetry and laboratory cross section plotted versus laboratory angle for the representative incident energy of 9.712 GeV.

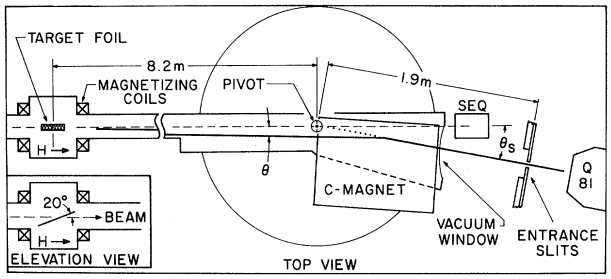

FIG. 2. Schematic outline of the experimental arrangement. The heavy line shows the typical trajectory of a scattered electron. Note that the trajectory after bending in the C magnet can be extrapolated (dotted line) through the spectrometer pivot point. The beam-line vacuum extends through the C magnet. Q81 is the first quadrupole in the 8-GeV/c spectrometer; SEQ is a secondary-emission quantameter used to monitor the beam.

trodynamic. Figure 1 shows the Møller asymmetry[8] and laboratory cross section[9] at the representative incident beam energy of 9.712 GeV. It should be noted that for this energy, a center-of-mass scattering angle ($\theta_{c.m.}$) of 90°, where the asymmetry reaches a maximum of $\frac{7}{9}$, corresponds to a laboratory angle of only 10 mrad. Thus any Møller-scattering apparatus must be able to separate physically the scattered electrons from the primary beam.

The experimental arrangement is shown in Fig. 2. The incident beam strikes a 0.025-mm-thick Supermendur[10] target foil located 8.2 m upstream from the pivot about which the spectrometer rotates. The foil is magnetized to saturation in a 90-G longitudinal magnetic field and is inclined at 20° to the beam in order to provide a large component of longitudinal polarization. Reversal of this 90-G field reverses the polarization of the target. The effective degree of electron spin polarization in the foil, measured by the emf induced in a pickup coil during magnetization reversal, is 0.083 ± 0.002. A C magnet, located downstream from the spectrometer pivot, separates the Møller-scattered electrons from the primary beam. The electrons which enter the 8-GeV/c spectrometer are deflected through angles between 6° and 10° while the primary beam is deflected by less than 2° in the fringe field. The C magnet is positioned so that the particles entering the spectrometer appear to originate from the center of the pivot at an angle θ_s from the primary-beam direction. Since the spectrometer normally views a target placed at this location, the spectrometer optics are unchanged from those applicable to a conventional high-energy experiment. The spectrometer determines the momentum, p, of particles to 0.2% in a 21-element scintillation-counter hodoscope; the angle θ_s is likewise measured to 0.3 mrad in a 55-element hodoscope. The vertical entrance aperture of the spectrometer (located 1.9 m from the pivot) is limited to ± 1 cm by a set of tungsten slits.

Particle identification is effected by means of a gas-filled threshold Cherenkov counter and a lead-Lucite shower counter. The two-body kinematics of Møller scattering ensures a nearly lin-

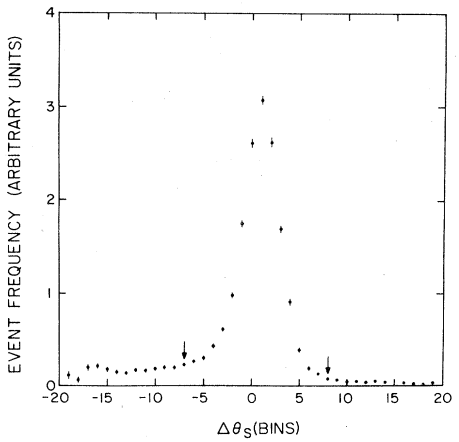

FIG. 3. Binned event frequency for a typical run (beam energy = 19.40 GeV, $\theta_{c.m.} = 128.5°$) plotted versus $\Delta\theta_s$, the deviation of the measured θ_s from the value predicted for e-e kinematics. Bin width is 3 mrad. The data have been corrected for the nonuniform acceptance in $\Delta\theta_s$. The region between the arrows was used to form the raw asymmetry listed in Table I.

TABLE I. Summary of polarization measurements. θ_a is the spin-momentum precession angle; A_{max} is the asymmetry expected for a fully polarized beam in the absence of non-Møller backgrounds; A_{raw} is the uncorrected asymmetry observed in the region indicated in Fig. 3; f is the fractional contamination due to non-Møller backgrounds; and $P = A_{raw}/A_{max}(1-f)$ is the longitudinal beam polarization averaged over both senses of source polarization.

E (GeV)	θ_a	$\theta_{c.m.}$ (deg)	A_{max}	A_{raw}	f	P
6.474	2π	75.5	0.0551	0.0286 ± 0.0017	0.33	0.768 ± 0.051
9.712	3π	90	0.0607	-0.0384 ± 0.0016	0.19	-0.784 ± 0.033
9.712	3π	120	0.0402	-0.0233 ± 0.0030	0.02	-0.588 ± 0.074
11.331	3.5π	99	0.0584	0.0009 ± 0.0028	0.15	0.018 ± 0.057
19.402	6π	128.5	0.0308	0.0224 ± 0.0025	0.07	0.785 ± 0.088

ear relation between θ_s and p for events within the small spectrometer acceptance. The background events, which arise mainly from radiative Coulomb scattering, are smoothly distributed in the (p, θ_s) plane. Figure 3 shows event frequency (corrected for detector acceptance) versus $\Delta\theta_s$, the deviation of θ_s from that value expected from two-body kinematics.

The experiment comprised a series of runs, each lasting about 1 h, during which the sense of source polarization was unchanged. The sign of the target polarization was reversed 50 times during each run in a $++--\ldots$ pattern of 100 "mini-runs." The number of events in each mini-run was converted to a cross section by normalizing to the charge collected by a secondary-emission quantameter. These data were corrected for electronic (~0.2%) and computer (~10%) dead times and for ambiguities in the p or θ_s hodoscopes (~3%). The 25 measurements of the "real" asymmetry and the 50 measurements of a "false" asymmetry which were extracted from each run showed nearly ideal statistical behavior.[11] Non-Møller backgrounds were dependent on kinematics and varied between 2% and 33% (see Table I).

The raw asymmetries, typically 0.03, were converted to beam polarizations by dividing by the factor $(1-f)A_M P_T$, where f is the ratio of the non-Møller events to the total number of events, A_M is the Møller asymmetry for fully polarized beam and target, and P_T is the longitudinal component of the target polarization ($P_T = 0.083 \cos 20°$).

The results, uncorrected for small spin-dependent radiative effects,[12] are summarized in Table I, and the longitudinal beam polarization is plotted as a function of beam energy in Fig. 4. Over the energy range studied, 6.47–19.4 GeV, the data are consistent with lowest-order quantum electrodynamic predictions for Møller scattering and with a longitudinal beam polarization of magnitude 0.76 ± 0.03, independent of energy and the sense of source polarization. The uncertainty in the polarization contains comparable contributions from statistics and from the target-polarization uncertainty, with a smaller contribution from uncertainty in the background correction. Finally, it is interesting to note that the experimental data shown in Fig. 4 are in excellent agreement (<1%) with the accepted value of the electron g-factor anomaly.

We gratefully acknowledge the technical support of M. Browne, D. Constantino, R. Eisele,

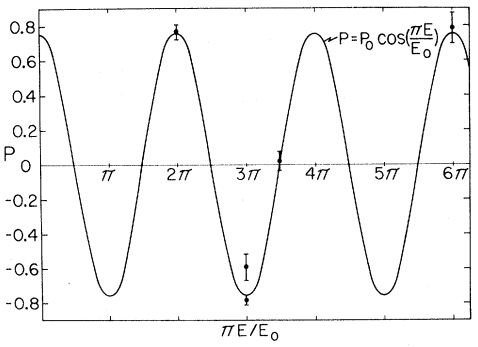

FIG. 4. The longitudinal component, P, of the beam polarization plotted versus $\pi E/E_0$, the angle through which the spin precesses relative to the momentum during the 24.5° bend into the experimental area. E is the beam energy and $E_0 = 3.237$ GeV. The curve shown is a best fit to the data and has an amplitude $P_0 = 0.76 \pm 0.03$. P_0 is the only free parameter.

R. Koontz, E. Taylor, L. Trudell, and the entire SLAC operations staff. We also wish to thank C. W. Tu for his assistance during the early stages of the experiments.

*Research (Yale Report No. COO-3075-90) supported in part by the U. S. Energy Research and Development Administration under Contract No. AT(11-1) 3075 (Yale) and Contract No. AT(04-3)515 (SLAC); the German Federal Ministry of Research and Technology and the University of Bielefeld; and the Japan Society for the Promotion of Science.

†Also at Nagoya University, Nagoya, Japan.

‡Also at Los Alamos Scientific Laboratory, Los Alamos, N. Mex. 87544.

§Also at University of Bielefeld, Bielefeld, West Germany.

‖Also at Yale University, New Haven, Conn. 06520.

[1]F. J. Gilman, SLAC Report No. 167, 1973 (unpublished), Vol. 1, p. 71.

[2]S. M. Berman and J. R. Primack, Phys. Rev. D 9, 217 (1974).

[3]SLAC Users Handbook (unpublished), Sect. D. 3

[4]M. J. Alguard *et al.*, in *Proceedings of the Ninth International Conference on High Energy Accelerators, Stanford, California, 1974*, CONF 740522 (Stanford Linear Accelerator Center, Stanford, Calif., 1974), p. 313.

[5]Calculations by W. P. Lysenko and R. H. Helm place an upper limit of 2.8% on the depolarization of the electron beam during acceleration to high energy; see also R. H. Helm and W. P. Lysenko, SLAC Report No. SLAC-TN-72-1, 1972 (unpublished).

[6]H. Frauengelder and A. Rossi, in *Methods of Experimental Physics*, edited by L. C. L. Yuan and C. S. Wu (Academic, New York, 1963), Vol. 5, Pt. B, p. 214.

[7]D. M. Schwartz, Phys. Rev. 162, 1306 (1967).

[8]A. M. Bincer, Phys. Rev. 107, 1434 (1957).

[9]See, for example, J. D. Bjorken and S. D. Drell, *Relativistic Quantum Mechanics* (McGraw-Hill, New York, 1964), p. 140.

[10]H. L. B. Gould and D. H. Wenny, Elec. Eng. (Amer. Inst. Elec. Eng.) 76, 208 (1967).

[11]The χ^2 statistic was evaluated for each run, in which 25 individual measurements of the asymmetry were combined to form a weighted mean. The χ^2 values for all the runs are in good agreement with the theoretical χ^2 distribution. Thus no evidence exists for nonstatistical fluctuations or drifts in monitors. In addition the false asymmetry formed from adjacent mini-run pairs of the same sign gave a result consistent with zero.

[12]L. L. DeRaad, Jr., and Y. J. Ng, Phys. Rev. D 11, 1586 (1975).

New Class of Bound-State Solutions in Field Theory

Paul Langacker*

Department of Physics, University of Pennsylvania, Philadelphia, Pennsylvania 1974

(Received 5 May 1975)

It is suggested that bound states can emerge in field theory as alternate solutions to the Bethe-Salpeter equation, not corresponding to the Neumann-series (perturbation-theory) solution. These new solutions are asymptotically similar to elementary-particle solutions and imply nonperturbative anomalous dimensions in the Wilson operator-product expansion. For Goldstone bosons in standard quark models as well as for certain solvable ladder models, these are the only bound-state solutions.

It is not at all clear that renormalizable field theories possess any bound states. The Bethe-Salpeter equation[1] (BSE) in the ladder approximation (Fig. 1) can sometimes be solved exactly[2-4] if one ignores the mass of the exchanged particle. These calculations yield branch points rather than Regge poles[5] for the t-channel partial-wave amplitudes at $q_\mu = 0$. Perturbation calculations[6] of the same class of diagrams indicate that these branch points are fixed.[7] This is disturbing because the Schrödinger equation, which possesses bound states and moving Regge poles, can be de-

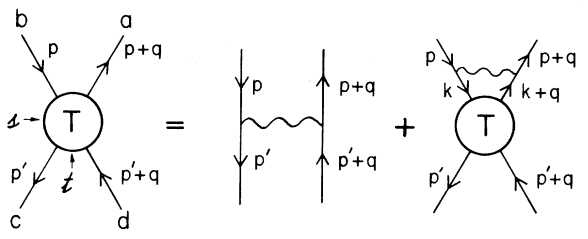

FIG. 1. The Bethe-Salpeter equation (BSE) for $T(p, p', q)$ in the ladder approximation. A bound state corresponds to a pole in T at $q^2 = m_B{}^2$. The bound-state vertex function $\varphi(p, q)$ satisfies the homogeneous BSE.